Unfavorable electrostatic and steric interactions in DNA polymerase β E295K mutant interfere with the enzyme's pathway

Yunlang Li†, Chelsea L. Gridley‡, Joachim Jaeger‡§, Joann B. Sweasy||

and Tamar Schlick*†

† Department of Chemistry and Courant Institute of Mathematical Sciences, New York University, 251 Mercer Street, New York, NY 10012

‡ Department of Biomedical Sciences, School of Public Health, University at Albany, 1400 Washington Avenue, Albany, NY 12222, USA

§ Division of Genetics, Wadsworth Center NYS-DOH, New Scotland Avenue, Albany, NY 12208, USA

|| Department of Therapeutic Radiology, Yale University School of Medicine, 333 Cedar Street, P.O. Box 208040, New Haven, CT 06520, USA

* To whom correspondence should be addressed (Phone: 212-998-3116; e-mail: schlick@nyu.edu; fax: 212-995-4152)

SUPPORTING INFORMATION

Protonation States

We choose protonation states of the titratable side chains and phosphate groups in pol β based on individual pKa values at a solution pH of 7.0 as reported in Table SIII. Because the three conserved Asp groups are well separated from each other and not closely interacting with the dCTP in the crystal structure, our choice of the protonation states based on pKa of the amino acid group and an overall pH of 7.0 is reasonable. It is also in accord with previous work[1,2]. We choose HID (His with hydrogen on the delta nitrogen) for all His groups. Note that none of the key residues around the active site are His, so this choice of His tautomers is expected to have have little impact on the results of this paper.

Shooting Algorithm and Test of Convergence of TPS

The shooting algorithm[3-5] generates an ensemble of new trajectories by perturbing initial momenta of atoms in a randomly chosen time interval while ensuring conservation of Maxwellian distribution of velocities, total linear and angular momentum, and detailed balance. The perturbation scheme employed in our work is also symmetric – the probability of generating a new set of momenta from the old set is the same as the reverse probability of generating the old set from the new set.

In particular, the ensemble of new trajectories $\{\chi_\tau\}$ of length τ are generated by a Metropolis algorithm according to a path action $S\{\chi\}_\tau$: $S\{\chi\}_\tau = \rho(0)\, h_A(\chi_0) H_B\{\chi\}_\tau$, where $\rho(0)$ is the probability of observing the configuration at $t = 0$ ($\rho(0) \propto \exp(-\beta E(0))$ in the canonical ensemble). The newly generated trajectories are accepted or rejected based on selected statistical criteria that characterize the ensemble of trajectories[3,6].

The ergodicity and convergence of each TPS run is confirmed by calculating the autocorrelation function of the order parameter $\langle \chi_i(0)\chi_i(\tau)\rangle$ associated with each transition state i, where $\langle\cdot\rangle$ denotes the average over the ensemble of generated trajectories. For each transition state, the autocorrelation function is plotted from time 0 where $\langle \chi_i(0)\chi_i(0)\rangle \approx \langle \chi_A\rangle^2$ to the time τ where $\langle \chi_i(0)\chi_i(\tau)\rangle \approx \langle \chi_A\rangle\langle \chi_B\rangle$; this range is spanned during our sampling time τ (see Supplemental Figure S2), indicating that the transition state regions between A and B are crossed during this interval. The time used for the gradual transition of the autocorrelation function $\langle \chi_i(0)\chi_i(\tau)\rangle$ from these plots can provide an estimate for the timescale of barrier crossing (τ_{mol})[7]. Thus, the length of the MD trajectories should be longer than the τ_{mol} value to sufficiently cover the entire transition region.

The above procedure both conserves the equilibrium distribution of individual metastable states and ensures that the accepted molecular dynamics trajectories connect the two metastable states for a particular transition. The shooting algorithm used in our work based on the Metropolis scheme also conserves microscopic reversibility. Hence, the ensemble of MD trajectories generated is guaranteed to converge to the correct ensemble defined by the path action and represents configurations that constitute the correct pathway for hopping between the metastable states.

References

(1) Radhakrishnan, R.; Schlick, T. *J. Am. Chem. Soc.* **2005**, *127*, 13245.

(2) Radhakrishnan, R.; Schlick, T. *Proc. Natl. Acad. Sci. U. S. A.* **2004**, *101*, 5970.

(3) Bolhuis, P. G.; Chandler, D.; Dellago, C.; Geissler, P. L. *Annu. Rev. Phys. Chem.* **2002**, *53*, 291.

(4) Dellago, C.; Bolhuis, P. G.; Geissler, P. L. *Advances in Chemical Physics, Vol 123* **2002**, *123*, 1.

(5) Bolhuis, P. G.; Dellago, C.; Chandler, D. *Faraday Discuss.* **1998**, *110*, 421.

(6) Radhakrishnan, R.; Schlick, T. *J. Chem. Phys.* **2004**, *121*, 2436.

(7) Chandler, D. *J. Chem. Phys.* **1978**, *68*, 2959.

(8) Vande Berg, B. J.; Beard, W. A.; Wilson, S. H. *J. Biol. Chem.* **2001**, *276*, 3408.

(9) Murphy, D. L.; Jaeger, J.; Sweasy, J. B. *J. Am. Chem. Soc.* **2011**, *133*, 6279.

(10) Yamtich, J.; Starcevic, D.; Lauper, J.; Smith, E.; Shi, I.; Rangarajan, S.; Jaeger, J.; Sweasy, J. B. *Biochemistry* **2010**, *49*, 2326.

(11) Murphy, D. L.; Kosa, J.; Jaeger, J.; Sweasy, J. B. *Biochemistry* **2008**, *47*, 8048.

(12) Dalal, S.; Hile, S.; Eckert, K. A.; Sun, K. W.; Starcevic, D.; Sweasy, J. B. *Biochemistry* **2005**, *44*, 15664.

(13) Dalal, S.; Kosa, J. L.; Sweasy, J. B. *J. Biol. Chem.* **2004**, *279*, 577.

(14) Shah, A. M.; Li, S. X.; Anderson, K. S.; Sweasy, J. B. *J. Biol. Chem.* **2001**, *276*, 10824.

(15) Liu, J.; Tsai, M. D. *Biochemistry* **2001**, *40*, 9014.

(16) Ahn, J. W.; Kraynov, V. S.; Zhong, X. J.; Werneburg, B. G.; Tsai, M. D. *Biochem. J.* **1998**, *331*, 79.

(17) Kraynov, V. S.; Werneburg, B. G.; Zhong, X.; Lee, H.; Ahn, J.; Tsai, M. D. *Biochem. J.* **1997**, *323 (Pt 1)*, 103.

(18) Ahn, J.; Werneburg, B. G.; Tsai, M. D. *Biochemistry* **1997**, *36*, 1100.

(19) Werneburg, B. G.; Ahn, J.; Zhong, X.; Hondal, R. J.; Kraynov, V. S.; Tsai, M. D. *Biochemistry* **1996**, *35*, 7041.

(20) Kraynov, V. S.; Showalter, A. K.; Liu, J.; Zhong, X. J.; Tsai, M. D. *Biochemistry* **2000**, *39*, 16008.

(21) Shah, A. M.; Conn, D. A.; Li, S. X.; Capaldi, A.; Jager, J.; Sweasy, J. B. *Biochemistry* **2001**, *40*, 11372.

(22) Li, S. X.; Vaccaro, J. A.; Sweasy, J. B. *Biochemistry* **1999**, *38*, 4800.

(23) Shah, A. M.; Maitra, M.; Sweasy, J. B. *Biochemistry* **2003**, *42*, 10709.

(24) Dalal, S.; Starcevic, D.; Jaeger, J.; Sweasy, J. B. *Biochemistry* **2008**, *47*, 12118.

(25) Kosa, J. L.; Sweasy, J. B. *J. Biol. Chem.* **1999**, *274*, 35866.

(26) Beard, W. A.; Shock, D. D.; Yang, X. P.; DeLauder, S. F.; Wilson, S. H. *J. Biol. Chem.* **2002**, *277*, 8235.

(27) Dalal, S.; Chikova, A.; Jaeger, J.; Sweasy, J. B. *Nucleic Acids Res.* **2008**, *36*, 411.

(28) Lang, T. M.; Dalal, S.; Chikova, A.; DiMaio, D.; Sweasy, J. B. *Mol. Cell. Biol.* **2007**, *27*, 5587.

(29) Eger, B. T.; Benkovic, S. J. *Biochemistry* **1992**, *31*, 9227.

(30) Wang, Y. L.; Schlick, T. *BMC Struct. Biol.* **2007**, *7*.

Supplementary Table

Table SI. Kinetic data for wild-type pol β and mutants with correct base-paring. See also Supplementary Figures S8 and S9.

	k_{pol} (s^{-1})	K_d (μM)	ΔG (kJ/mol)[a]
Wild-type [8-20]	3 – 54	2.5 – 63	64.1 – 71.3
N279A[b 17]	44 ± 10	1400 ± 600	64.2 ± 0.29
M282L[b 21]	39.8 ± 4.6	92 ± 28	64.4 ± 0.14
D246V [13]	31.8 ± 2.6	29.1 ± 6.2	65.0 ± 0.10
F272L[b 22]	30 ± 1	77 ± 10	65.1 ± 0.04
Y265W[b 23]	19.4 ± 0.3	14 ± 1	66.2 ± 0.02
Y265F[b 23]	18.2 ± 0.9	63 ± 11	66.4 ± 0.06
N279Q[b 17]	14 ± 2	610 ± 120	67.0 ± 0.18
K280A [20]	12	6	67.4
R149A [20]	11	12	67.6
I260Q[b 24]	10.8 ± 1.5	165 ± 40	67.7 ± 0.17
E249K [25]	9.1 ± 0.5	25 ± 4	68.1 ± 0.07
S188A[b 20]	8.9	3.8	68.1
D276R[b 15]	8.6 ± 0.87	170 ± 30	68.2 ± 0.13
I174S [10]	6.7 ± 0.7	23 ± 6	68.8 ± 0.13
D276V [8]	6.3 ± 0.9	0.6 ± 0.3	69.0 ± 0.18
N294A [20]	4.0	6.6	70.1
Y271F [17]	3.30 ± 0.35	3.7 ± 1.2	70.6 ± 0.13

K280G[b] [26]	2.7 ± 0.1	289 ± 26	71.1 ± 0.05
R183A [20]	2.6	5.9	71.2
N294Q [20]	2.6	1.6	71.2
H285D [11]	2.5 ± 0.2	4.4 ± 0.9	71.3 ± 0.10
E295A [20]	2.0	10	71.8
I260M [12]	2.0 ± 0.1	6 ± 1	71.8 ± 0.06
S180A[b] [20]	1.0	70	73.5
Y271S [17]	1.0 ± 0.1	4.7 ± 0.5	73.5 ± 0.12
R283A [18]	0.83 ± 0.08	61 ± 17	74.0 ± 0.12
Y271A [17]	0.58 ± 0.03	1.4 ± 0.2	74.9 ± 0.06
Y265H[b] [14]	0.087 ± 0.003	1.2 ± 0.1	79.6 ± 0.04
R333E [9]	0.074 ± 0.003	70 ± 9	80.0 ± 0.05
R283K[b] [19]	0.05 ± 0.01	170 ± 60	81.0 ± 0.25
R182E [9]	0.034 ± 0.002	131 ± 19	81.9 ± 0.07
E316R [9]	0.00185 ± 0.00006	20 ± 4	89.1 ± 0.04
L22P [27]	(No activity)	291 ± 45	N/A
E295K [28]	(No activity)	28	N/A

a. k_{pol} is the intrinsic rate constant of polymerization, K_d is the equilibrium dissociation constant for the incoming nucleotide. ΔG is the overall energy barrier in pol β's catalytic pathway and is calculated as $\Delta G = RT\,[\ln(k_B T/h) - \ln(k_{pol})]$[29], where R is the universal gas constant and h is the Planck constant.

b. N279A, F272L, N279Q, I260Q, S188A, K280G, S180A, and Y265H are measured with a base-paring of A:dTTP; M282L,Y265W, Y265F , D276R, and R283K are measured with a base-paring of T:dATP; all other mutants and the wild-type pol β are measured with a base-paring of G:dCTP. See Supplementary Figure S8 for a

summary of pol β's mutants, and Supplementary Figure S9 for the locations of the residues.

Table SII. Sequence of transition states for the closing conformational profiles of five pol β systems identified by TPS.

	E295K mutant	Wild-type (G:C)	Wild-type (G:A)	Wild-type (8-oxoG:C)	Wild-type (8-oxoG:A)
TS1	Flip of Asp192	Thumb closing	Thumb closing	Thumb closing	Thumb closing
TS2	Thumb closing	Flip of Asp192	Flip of Asp192	Arg258 half-rotation	Flip of Asp192
TS3	Flip of Phe272	Arg258 rotation	Flip of Phe272	Arg258 full-rotation	Arg258 rotation
TS4	Arg258 rotation	Flip of Phe272	Arg258 rotation	Flip of Phe272	Flip of Phe272
TS5	Shift of Tyr271	Ion motions			
TS6	Ion motions				

Table SIII. Protonation states of titratable side chains and phosphate groups in pol β.

Residue	Charge	pKa
Phosphate groups in DNA	–1	1.2
Asp	–1	3.9
Glu	–1	4.3
His	0	6.5
Lys	+1	10.8
Arg	+1	12.5

Supplementary Figures

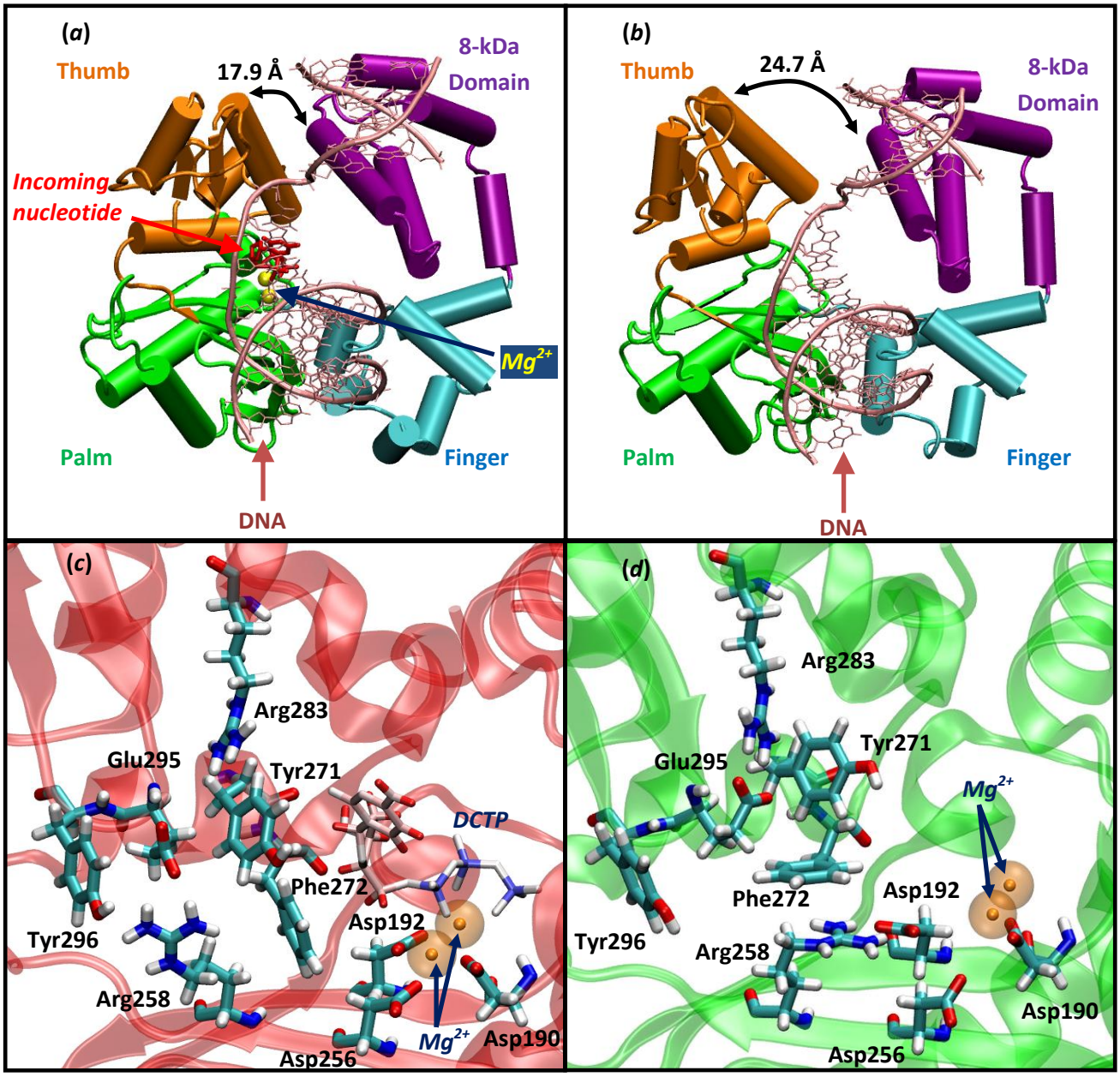

Fig. S1. Open-closed transition of pol β revealed in crystal structures.

Upper: Crystallographic pol β conformations before chemistry in (a) closed (PDB entry 1BPY) and (b) open (PDB entry 1BPX) forms. The distances between thumb and 8-kDa domain are shown.

Lower: Active site coordination of pol β before chemistry in (c) closed and (d) open forms.

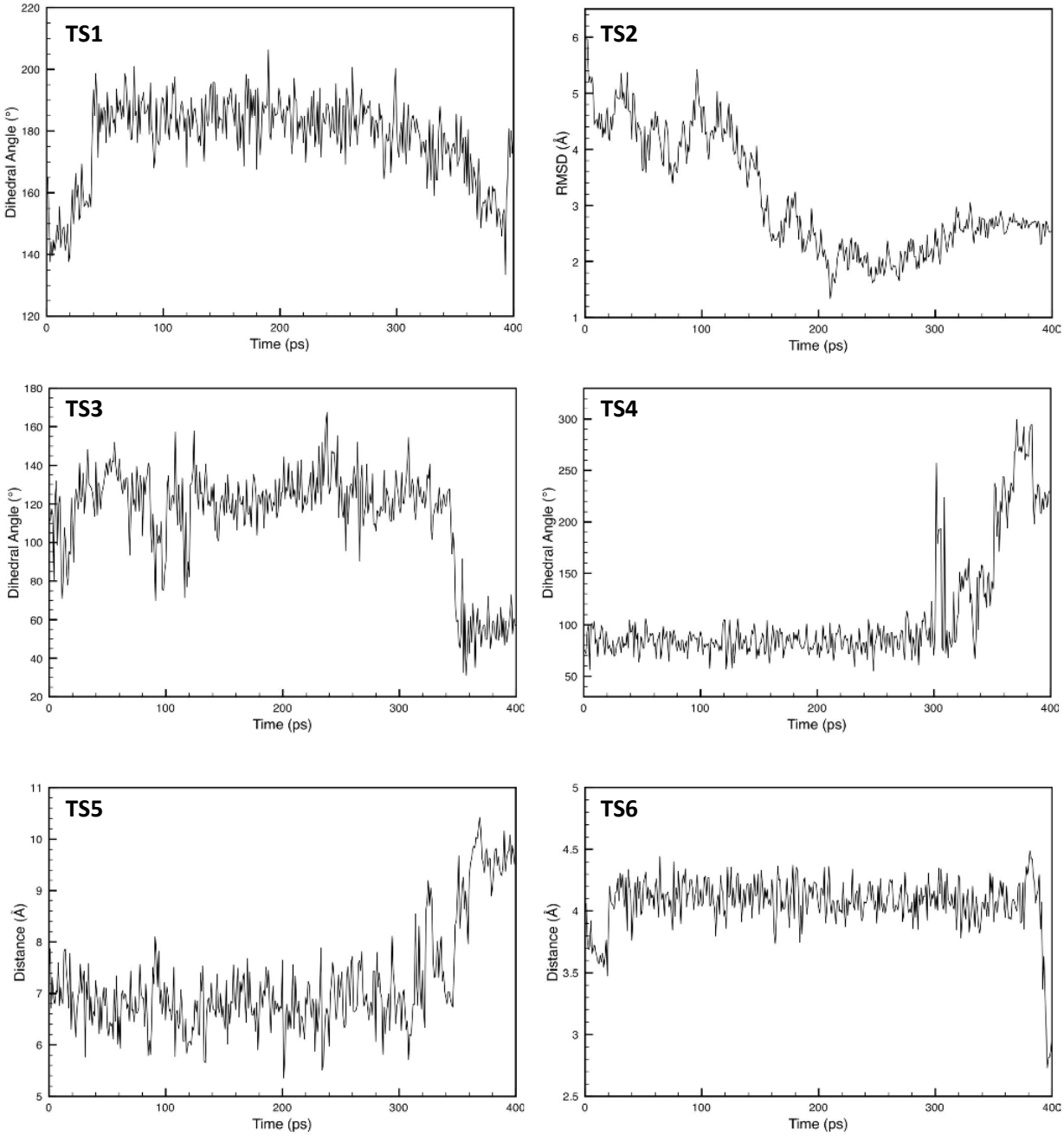

Fig. S2. Initial constrained trajectories for the conformational transitions obtained from TMD.

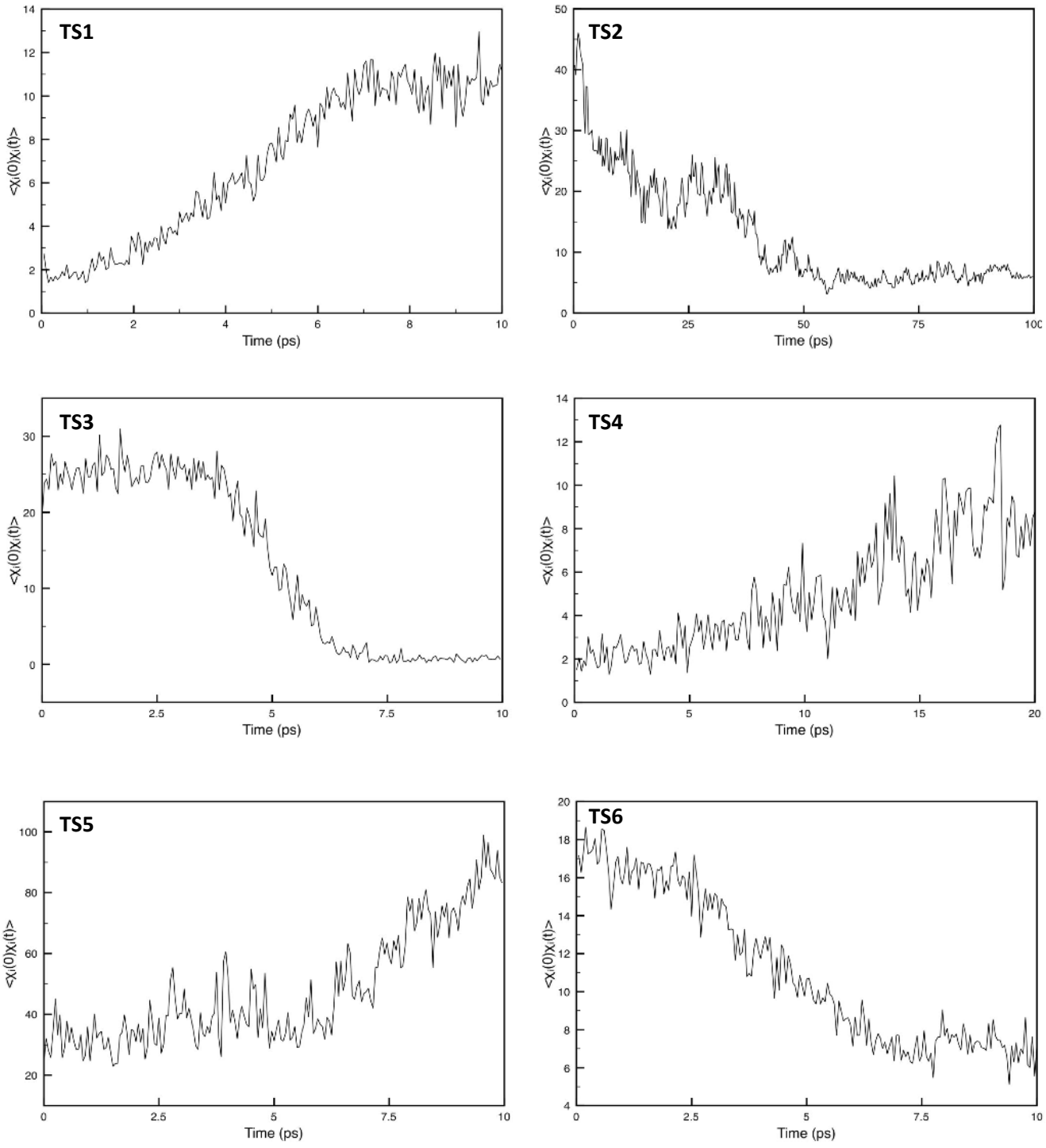

Fig. S3. Correlation functions of order parameters for transiton states in the closing pathway.

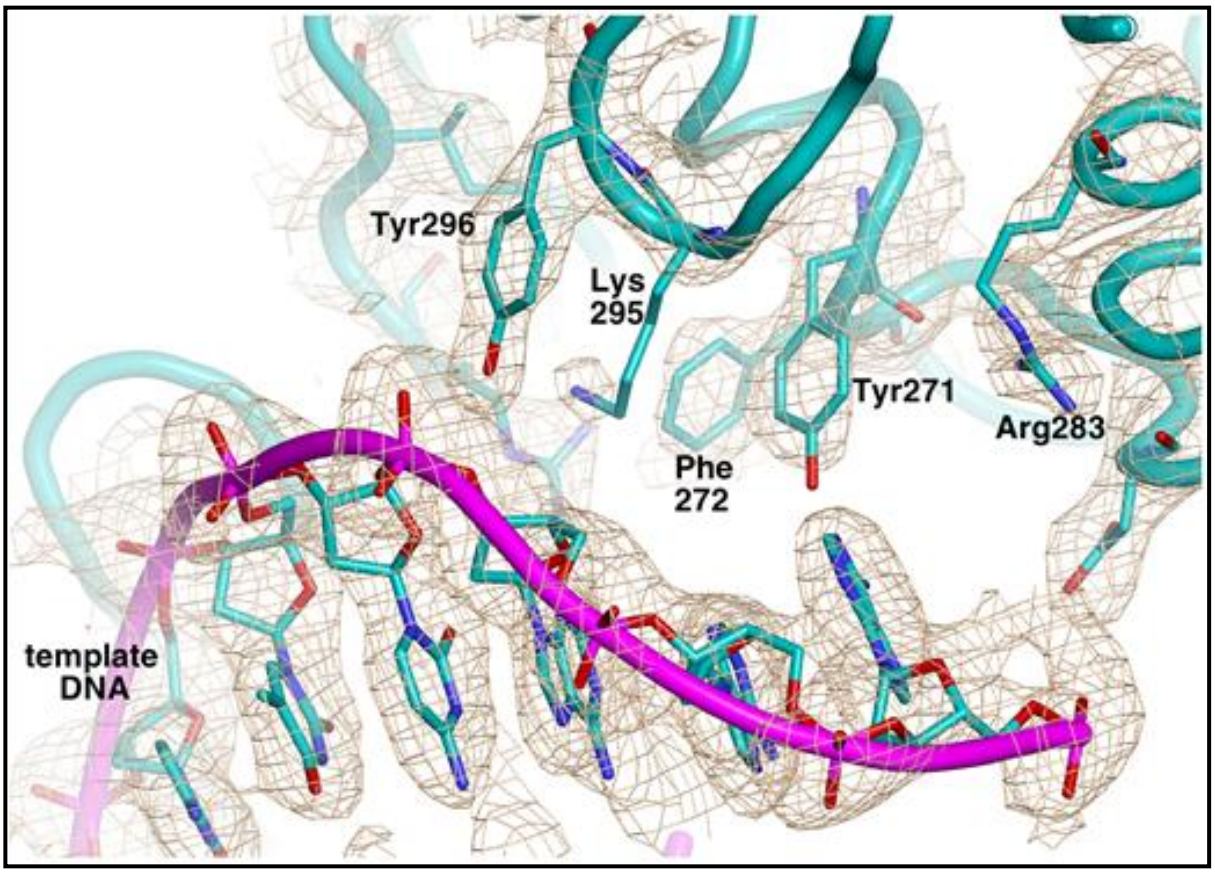

Fig. S4. Electron density map of the pol β E295K binary complex contoured at 1.25 RMS above the mean. The final model is superimposed in stick representation. Note the lack of electron density for Lys295.

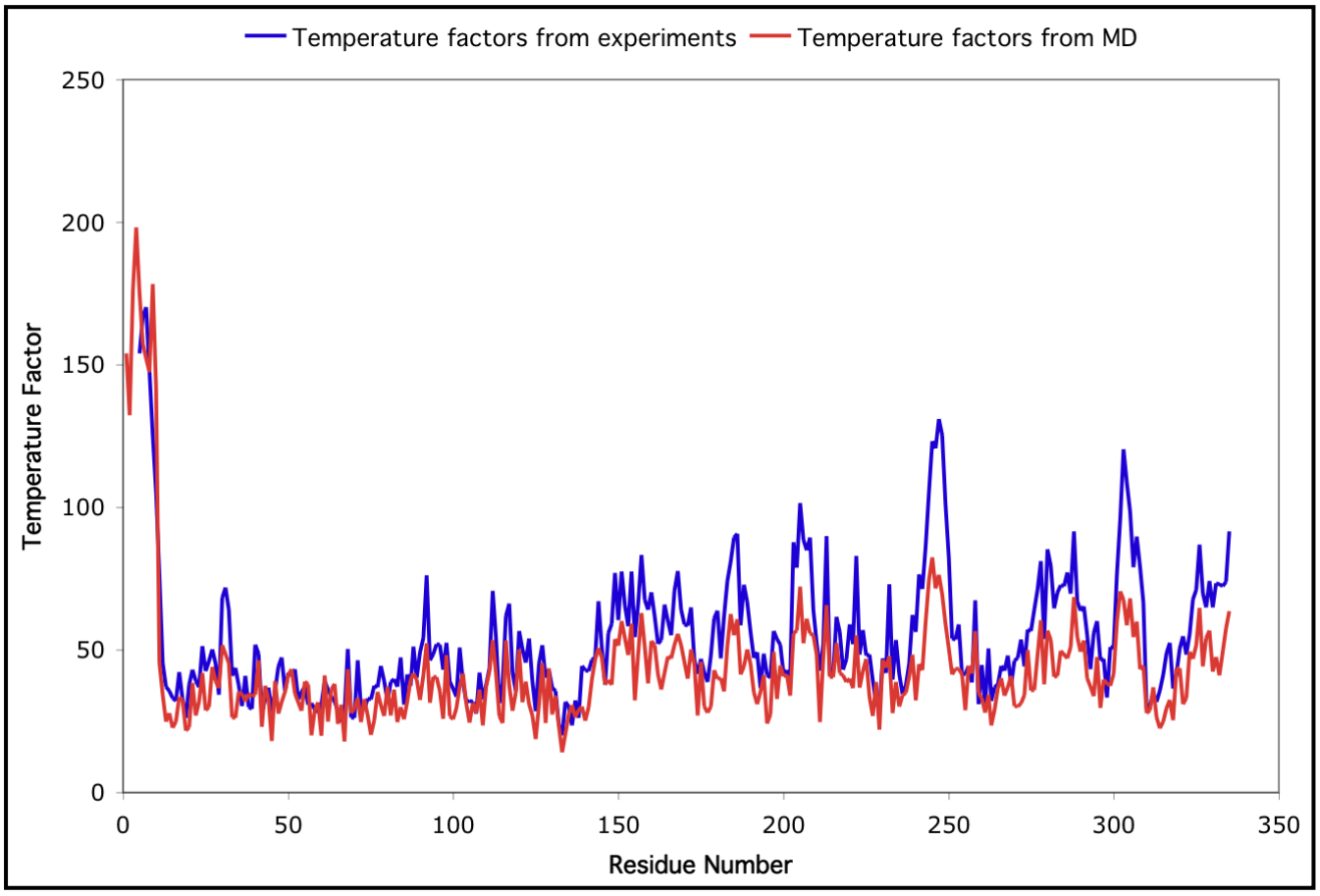

Fig. S5. Comparison of temperature factors of Cα atoms from experiments and from MD simulations.

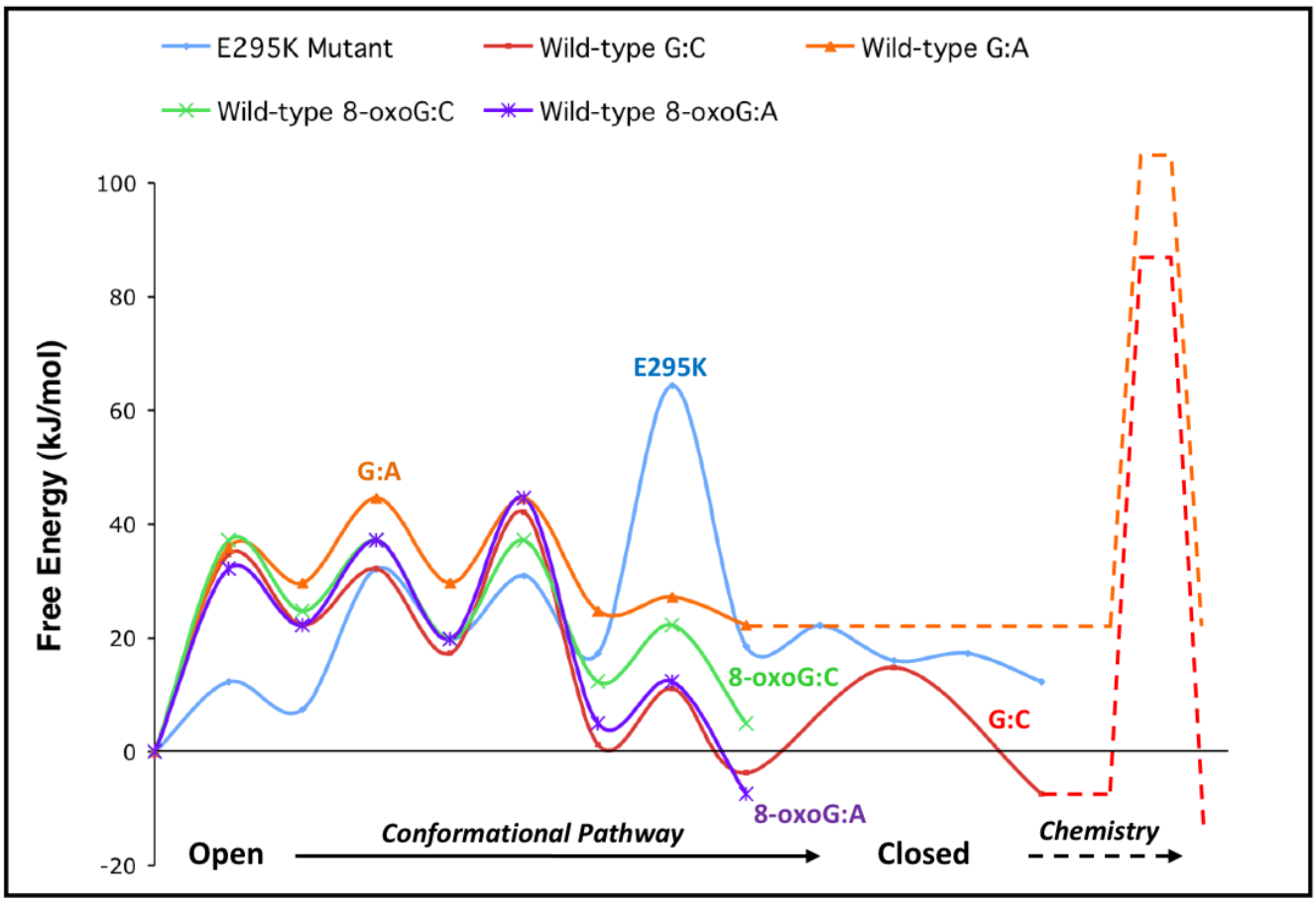

Fig. S6. Superimposed free energy profiles of five pol β systems obtained from TPS[1,2,30]. The energy barrier of the chemical step for wild-type G:C and G:A are also shown in dashed lines, which are derived from experimentally measured k_{pol} values[8,14,16,17,20]. See supplementary table II for the sequence of transition states in each system.

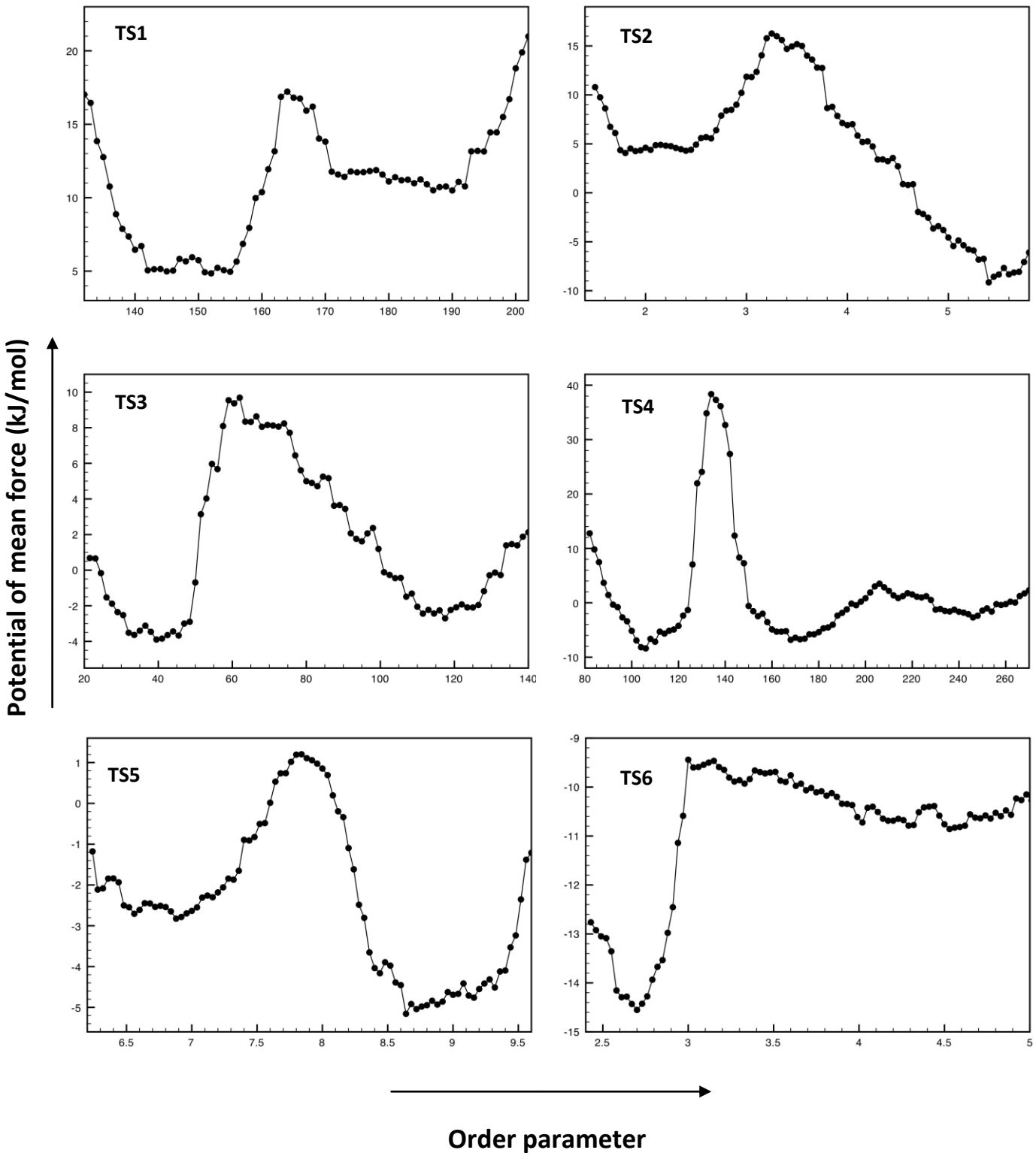

Fig. S7. Potential of mean force plots computed by BOLAS.

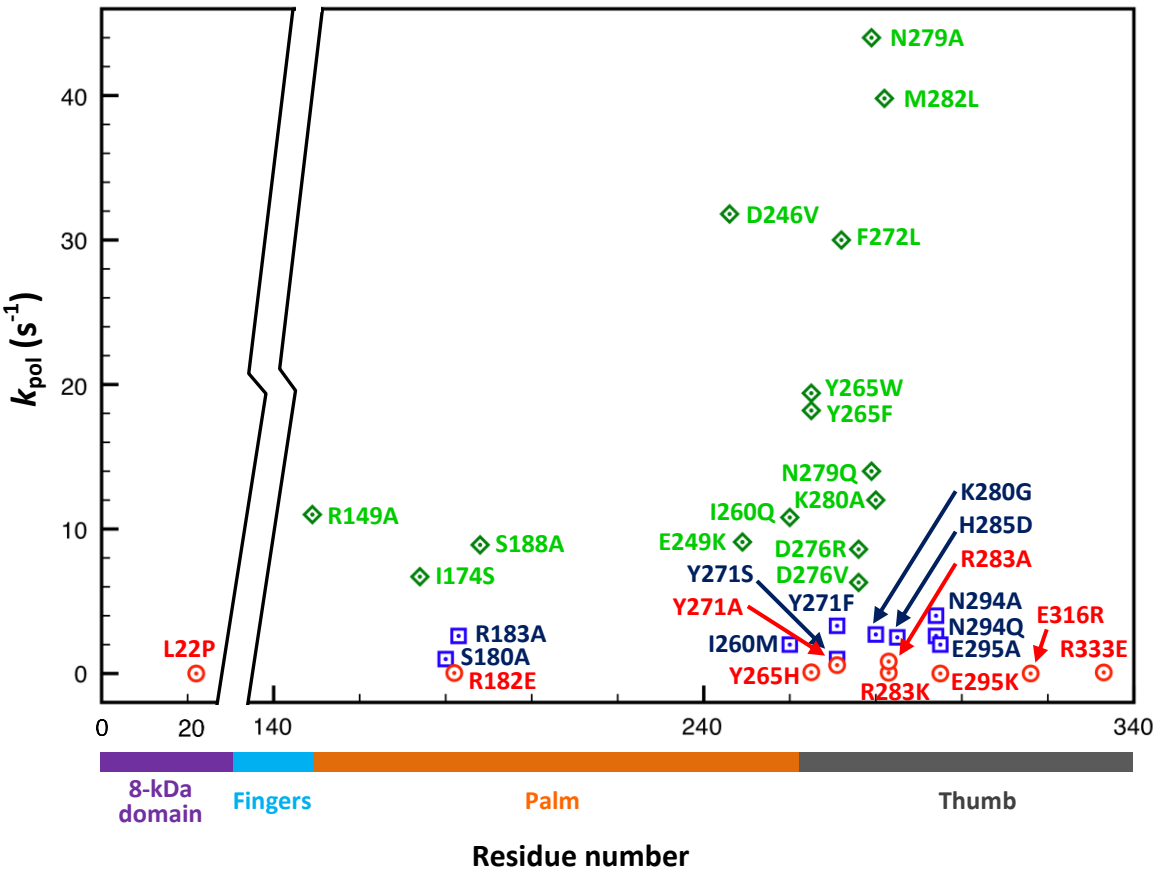

Fig. S8. Summary of activity of pol β's mutants. Green, active (k_{pol} > 4 s^{-1}); blue, activity reduced (k_{pol} between 4 s^{-1} and 1 s^{-1}); red, lost activity (k_{pol} < 1 s^{-1} or cannot be measured). See also Fig. S9.

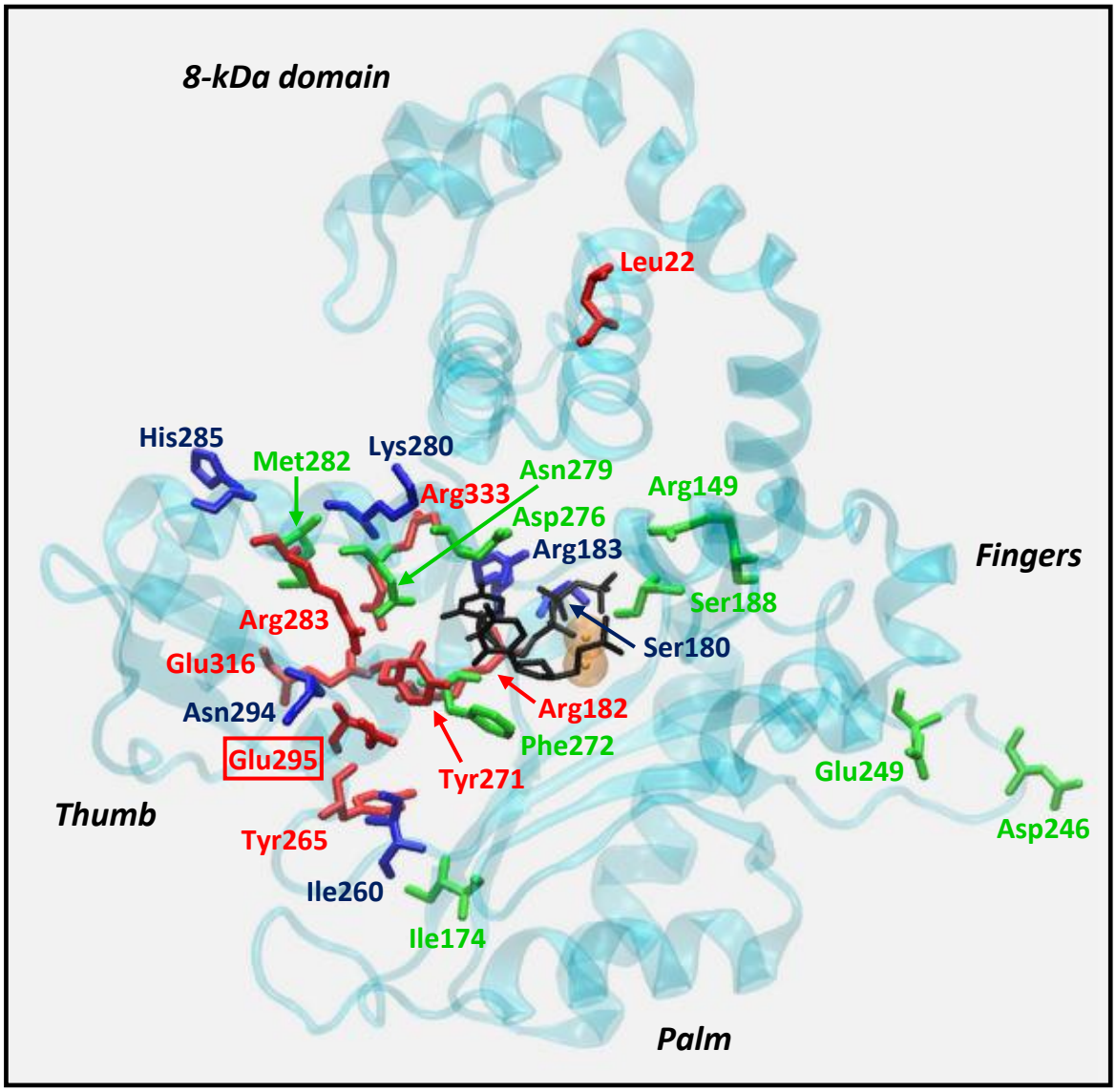

Fig. S9. Locations of residues listed in Table SI grouped by their effect on the enzyme's activity when mutated. If on the same residue, different mutations change pol β's activity differently, that residue is grouped according to the lowest activity of all the mutants on it. Green, blue, and red as in Fig. S8. Black, dCTP and C10; orange, Mg^{2+}.